

# Detection and Analysis of Bacterial Water using Photonic Crystal Ring-Resonator Based Refractive-Index Sensor on SOI Platform

Rohit Kumar<sup>1</sup>, Gaurav Kumar Bharti<sup>2</sup> and Ranjit Kumar Bindal<sup>3</sup>

<sup>1,2,3</sup>Department of Electrical Engineering, Chandigarh University, Mohali, India, <sup>1</sup>rohit.ee@cumail.in,

<sup>2</sup>gauravkumarbharti7@gmail.com, <sup>3</sup>ranjitbindal.eee@cumail.in

\*Correspondence: Rohit Kumar; Email: rohit.ee@cumail.in

**ABSTRACT-** A refractive-index biosensor is modeled using a photonic crystal ring resonator. The proposed sensor possesses a high selectivity and high quality-factor against different bacterial water samples. The introduction of the circular rim in the ring resonator structure is responsible for a sharp resonance that makes it suitable for detecting bacterial impurities. The sufficiently separated resonant peak for different samples offers a possibility of highly selective label-free bacterial water detection. The proposed biosensor is highly sensitive, real-time, lab-on-chip, and label-free, which is necessary for on-site detection. The proposed sensor is designed using a silicon-on-insulator platform.

**General Terms:** Silicon-On-Insulator, Lab-on-Chip, Label-Free Detection, Refractive-Index.

**Keywords:** Bacterial-Water Detection, Optical Biosensor, Photonic-Crystal, Refractive-Index Sensor, Ring Resonator.

## ARTICLE INFORMATION

**Author(s):** Rohit Kumar, Gaurav Kumar Bharti and Ranjit Kumar Bindal;

**Received:** 23/07/2022; **Accepted:** 30/09/2022; **Published:** 18/10/2022;

**e-ISSN:** 2347-470X;

**Paper Id:** IJEER-RDEC4279;

**Citation:** 10.37391/IJEER.100411

**Webpage-link:**

<https://ijeer.forexjournal.co.in/archive/volume-10/ijeer-100411.html>



**Publisher's Note:** FOREX Publication stays neutral with regard to Jurisdictional claims in Published maps and institutional affiliations.

## 1. INTRODUCTION

Photonic sensing technology is versatile and shows excellent reliability than its electronic counterparts. Optical biosensors have been used for medical diagnosis, detection of harmful pathogens and impurities [1-3]. Optical sensing is very significant especially in the field of light-analyte interaction as well as in its miniaturization. To realize a real-time as well as label-free detection technique, different optical sensors have been proposed based on slot waveguides [1], nano-cavity [2], micro-ring resonators [3], gratings-based devices [4], surface plasmon technique [5], photonic crystal-based structures [6], digital holographic microscopy (DHM) [7], and light scattering measurement (LSM) [8]. DHM and LSM suffer from less accuracy, while surface plasmon techniques are restricted by long acquisition time and low throughput. The surface-plasmon resonance sensors require a relatively huge sensing area. The refractive index (RI) based sensors control, handles, and efficiently analyze bacteria in a liquid medium [6], [9]. One of the primary impurities in drinking water is bacterial toxification, like *Vibrio cholera*, *Escherichia coli* (E. coli), *Shigella flexneri*, and *Salmonella enterica* [9].

These bacteria are frequently transferred via oral-fecal route and responsible for the amalgamation of food poisoning, vomiting, diarrhea, fever, and abdominal pain [9]. In the year 1998, 2000,

2008, an epidemic due to drinking water contamination happened in various parts of the world [9]. The technique used for the detection of contaminated water with bacteria is the United States Environmental Protection Agency (USEPA) based method which comprises of four stages - sample assembly, pre-concentration, bacteria culture, and detection [9]. This method requires on-site monitoring as laboratory-based infrastructure is vital for bacteria culture and colony inspection, which requires a long processing time of at least 10 hours. The other method, called Polymerase chain reaction (PCR) method, is specific as well as faster than the USEPA method, which requires a three-step in vitro technique [10]. However, PCR detection is limited to detect the presence of bacteria in the water sample due to signal interference. Another method is immunoassay (ELISA method), which utilizes antigen-antibody reaction detection [10]. The ELISA method is relatively fast and has very low sensitivity. Thus, above all existing technique is not suitable for on-site detection. In order to avoid bacteria outburst, a real-time, sensitive, lab-on-chip, and label-free biosensor is needed.

Photonic crystals (PhCs) have improved towards device miniaturization with the goal of realizing lab-on-chip sensors. PhCs are the periodic arrangement of dielectric materials which possess characteristic optical gaps. PhCs sensors are utilized for chemical, physical, biochemical detection, and for sensing in biomedical applications due to its ability to offer resilient light detention within the analyte [11]. Consequently, light has been focused in a very lesser volume, leading to a sufficient light-liquid interaction making the sensors sensitive to small (refractive index) RI deviations due to biological species immobilization [12]. The analysis is label-free and does not require markers. The performances of the proposed sensor can be improved by optimizing the setup of the device, such as coupling enhancement, the temperature stabilization, and the geometry of the device (such as the architecture, and the size of the rods).

In this paper, the RI based biosensor is proposed. In the proposed device, small volume of sample are only required and are sensed in their natural form. Further, RI is measured, which is induced by the molecular interactions [2], [4], [13]. The proposed lab-on-a-chip RI biosensor is able to detect various species of bacteria in water.

## 2. PROPOSED SENSOR DESIGN

The design of the proposed bio-sensing platform consists of two-dimensional pillar type PhC square lattice structure of silicon (Si) rods. on Silicon-on-Insulator (SOI) platform. This configuration is preferred to reduce the problems associated with absorption and material dispersion [2]. Distance between centers of two neighboring rods is  $0.54 \mu\text{m}$  well-known as lattice constant ( $a$ ), radii of Si rods are  $r = 0.2a$  ( $0.1 \mu\text{m}$ ). Periodic dielectric-air structure provides lateral confinement, and SOI structure provides vertical confinement. The dimension of the SOI slab is  $55 \mu\text{m}^2$ .

Photonic Band Gap (PBG) is calculated to determine the transmission spectra, and the two TM PBGs are found using Plane Wave Expansion (PWE) method [14]. In figure 1, the PBG for normalized frequency of  $0.43415$  to  $0.29024$  i.e.,  $1.243 \mu\text{m}$  to  $1.860 \mu\text{m}$  is shown which is suitable for proposed sensor designing. On introducing point defect and line defect, a ring resonator (RR) structure is formed, and light is localized.

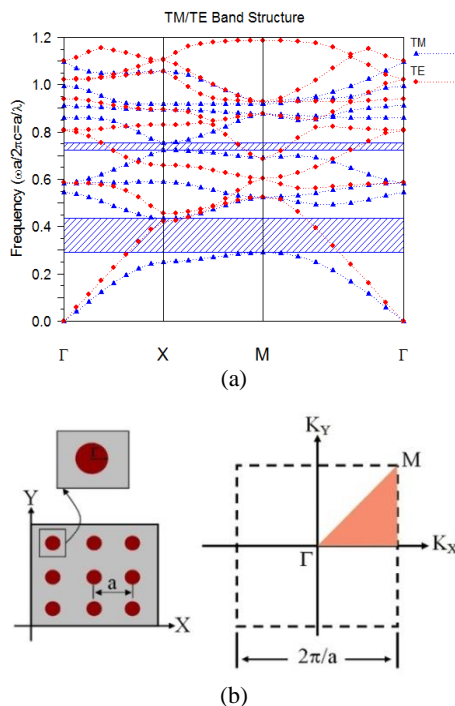


**Figure 1:** (a) Photonic crystal band gap for the proposed structure  
(b) Respective Brillouin zone of the square lattice

The electromagnetic wave propagation modes in PhC analysis follow Maxwell's equations [15]:

$$\nabla \times \left( \frac{1}{\epsilon(r)} \nabla \times E(r) \right) = \frac{\omega^2}{c^2} E(r) \quad (1)$$

Where  $\omega$  and  $E(r)$  are the angular frequency and dielectric function respectively,  $E(r)$  represents the field of the structure. From the above eq. 1, the 2D band structure is determined. The layout of the proposed model is shown in figure 2 (a)-(c).

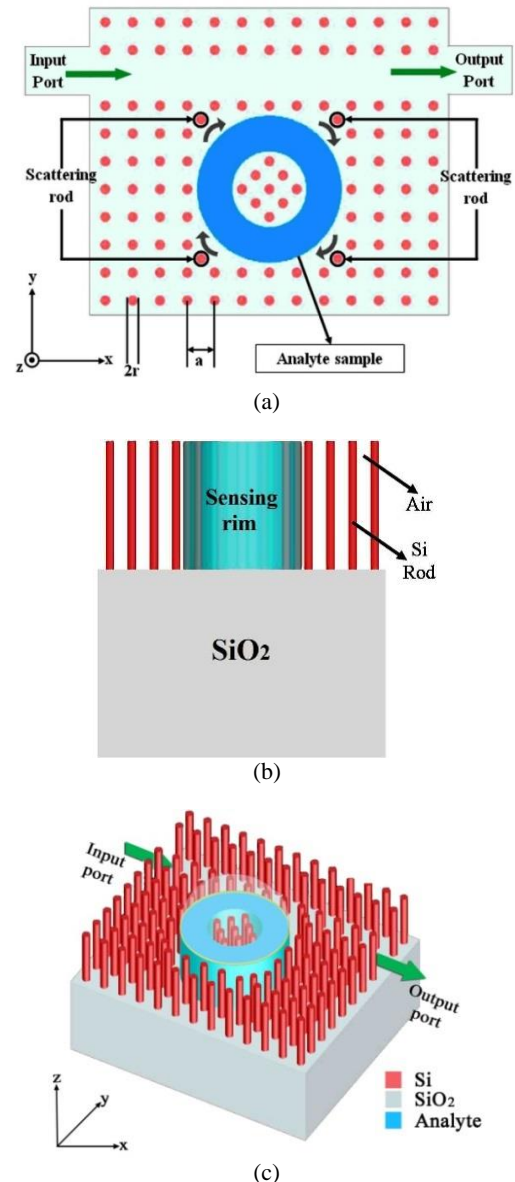


**Figure 2:** Proposed sensor system (a) Top view (b) Side view (c) Perspective view

The input source is set at the center wavelength of  $1500 \text{ nm}$ . For enhanced response and sensitivity, the inner rods are placed in a diamond-shaped manner. Scattering rods are employed in the ring to avoid significant scattering losses and capable to improve the spectral selectivity [3]. The optimized coupling length of about  $2800 \text{ nm}$  is selected. The proposed architecture enables more coupling length than an ideal waveguide-based ring structure which helps in better accumulation of light intensity. All the parameters like  $a$ ,  $r$ , etc. are optimized through numerical simulation. The ' $a$ ' and ' $r$ ' are tuned to obtain a resonance peak in the desired frequency range which is shown in figure 3. The finite-difference time-domain (FDTD) technique has been used to study the sensing capacity, spatial

mode profiles, etc [16]. The circular rim of RR is treated as the sensing area and it filled with samples for detection. With a change in the sample, the resonance wavelength shifts.

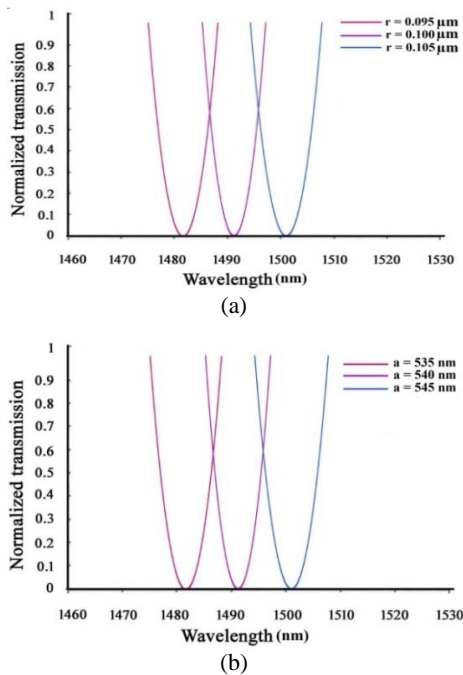


**Figure 3:** Response on transmission with the variation of (a) r (b) a

By examining the resonance shift, the sample filled in the sensing area can be derived using the monitor placed at the output port, as shown in *figure 2 (a)*. When light passes through a single bacterium in the sensing area, with air in the surrounding medium, the light rays are slowdown compared to the background medium. The interface of light and matter will be enriched; thereby, the absorption coefficient can be greatly improved, as given in *eq. (2)* [17].

$$\gamma \sim fc/v_g \quad (2)$$

Where  $\gamma$  is a dimensionless quantity which represents light enhanced absorption,  $f$  represents filling factor of the optical field,  $c$  is the speed of light in vacuum, and  $v_g$  is the group velocity of the input light. To reduce the optical loss occurred due to group index mismatch, the square lattice pattern of the cavity is changed in the proposed device. The parameter used for modelling the device is given in *table 1*.

**Table 1: Description for Modeling the Sensor**

Parameter	Description
Configuration	Rods in air
Lattice	Square
Source	1.40 $\mu\text{m}$ - 1.60 $\mu\text{m}$
Radius of Si rods (r)	100 nm
Lattice constant (a)	540 nm
Height of the rods (h)	360 nm
Substrate	SiO <sub>2</sub>
Height of substrate	3 $\mu\text{m}$
Footprint	55 $\mu\text{m}^2$

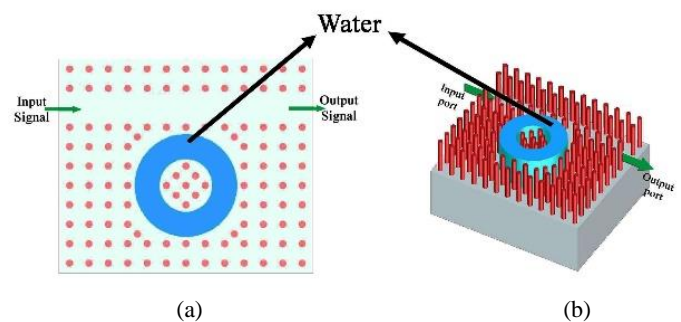
### 3. SIMULATION RESULTS

In operation, the input signal of gaussian pulse of TM mode with center wavelength 1500 nm is launched into the sensor system. The normalized transmission spectra at the output are achieved by 'Fast Fourier Transform' (FFT), computed by 2D-FDTD method [18].

The simulation region is bounded by the 'perfectly matched layer' (PML) which absorbs the field leaving in the simulated region and prevents reflections. The sample for detection is introduced from the top of the proposed system by the microfluidic channel, which supply the sample to the sensor and then to the waste solution bottle. The preliminary investigation is performed by supposing the intrusion of de-ionized (DI) water as a reference, which shows the alteration of RI from 1 (air) to 1.33 (DI water) [9], [15]. When the sample is changed, it binds inside the sensing region of the device and the local RI of the cavity changes and causes a resonant wavelength shift. *figure 4 (a)-(b)* shows the schematic of the model if the sensing area is filled with sample of DI water. The wavelength response of the sensor is shown in *figure 4 (c)*, and the inset shows the electric field localization in the vicinity of the spatial defects. The RI of the different samples is given in *table 2*.

In this paper, four different bacteria are detected in the sample of water. The grey, pink, blue, and yellow represent the presence of different bacteria in the sensing region, as shown in *figure 5(a) - (d)*. *Figure 6 (a) - (d)* shows transmission curve.

The electric field evolution of the sensing region for different bacterial water is shown in the inset of each figure which approves that the mode is restricted within the PhC RR. The light that permits through the device from one end will interact with the bacterial component of the sample and get detected from the other end. The alterations in the transmission wavelength are observed with the change of different samples in the sensing area. Depending on the RI of the bacterial sample which changes according to the type of bacteria existing in it, the transmission of the light will differ in the device. The resonant wavelength ( $\lambda_0$ ) in the transmission is marked in *table 2*, which shows the shifts towards the longer wavelength, i.e., the red-shifted behavior. The average diameter of the bacteria Vibrio Cholera, E. Coli and Shigella flexneri is 0.43  $\mu\text{m}$ , 0.57  $\mu\text{m}$  and, 0.77  $\mu\text{m}$  respectively, which can easily sustain in the sensing rim of diameter 1  $\mu\text{m}$  [9-10].





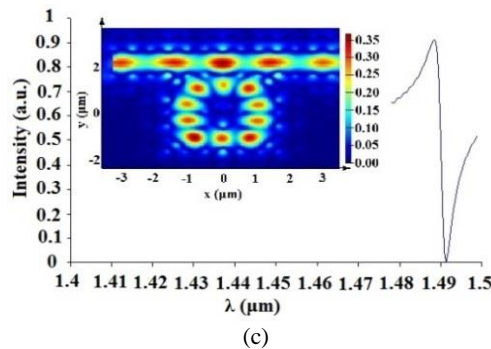


**Figure 4:** (a)-(b) Schematic layout of sensor for DI water detection (c) corresponding output response

**Table 2: RI considered and Resonant Wavelength Obtained for Different Samples during Simulation**

Noted value	DI water	Vibrio Cholera	E Coli	Shigella flexneri	Salmonella
RI	1.330 [9],[15]	1.365 [9]	1.390 [9], [11]	1.420 [9]	1.430 [10], [19]
$\lambda_0$	1.491 $\mu\text{m}$	1.514 $\mu\text{m}$	1.531 $\mu\text{m}$	1.552 $\mu\text{m}$	1.559 $\mu\text{m}$

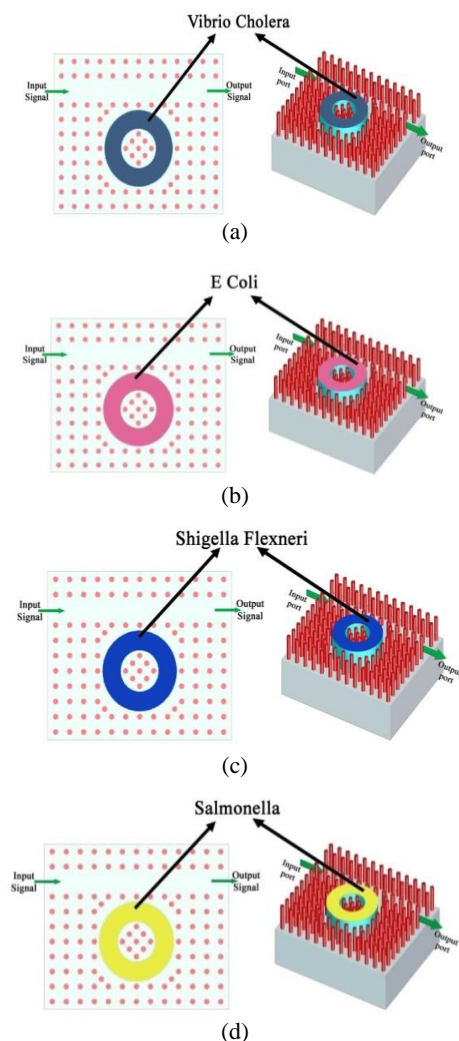


**Figure 5:** Schematic layout of the sensor for (a) Vibrio Cholera bacteria (b) E. Coli (c) Shigella Flexneri (d) Salmonella

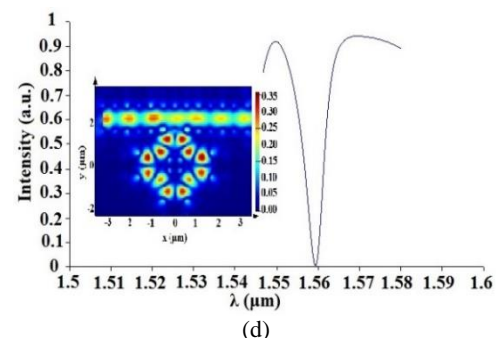
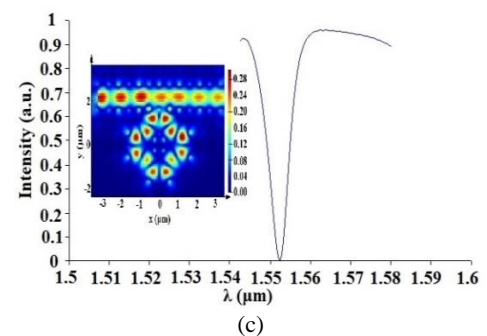
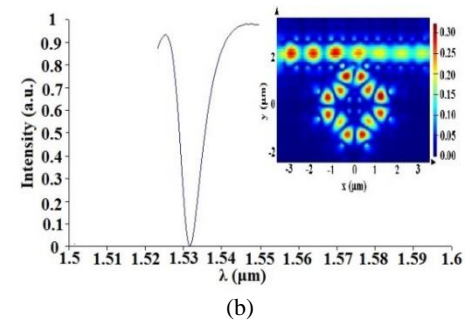
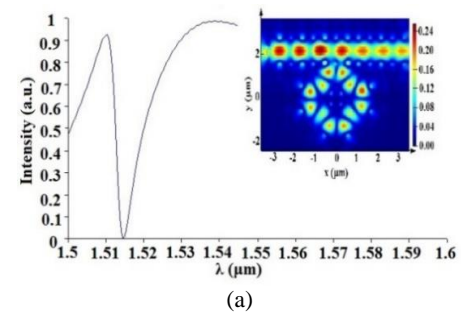


**Figure 6:** Transmission curve for (a) Vibrio Cholera bacteria (b) E. Coli (c) Shigella Flexneri (d) Salmonella. Electric field evolution in the inset

## 4. DISCUSSIONS AND PERFORMANCE ANALYSIS

The detection properties of the proposed device is predicted by the sensitivity parameter  $[S = (\Delta\lambda/\Delta n)]$ , where  $\Delta\lambda$  denotes wavelength-shift and the RI change occurred due to the sample infiltration is denoted by  $\Delta n$ . According to the proposed outputs, the  $\lambda_0$  is 'red-shifted' due to the rise in the effective RI of the region, this helps for the determination of the sample. The average sensitivity of 687nm/RIU is obtained for the proposed device. The value symbolizes larger Figures of Merit (FOM)

than other reported works which is given in *table 3* [20]-[22]. *Figure 6* shows the resonant dip corresponding to the bacterial infiltration due to low Full Width Half Maximum (FWHM), and therefore the extraordinary  $Q$  factor has been obtained. The average value of 1130.8 is obtained as a  $Q$  factor for the proposed sensor. The calculated  $Q$  factor and the FWHM of all five samples are mentioned in *table 3*.

The good performances of sensor are characterize by low Limit of Detection (LoD), which is defined as  $LoD = \lambda_0/Q.S$  [23]. The switching time of 42 fs is obtained for the proposed model. The overall size of the device is  $55 \mu m^2$ .

The results of this proposed work is compared with the previously published reports and shows significant improvements as shown in *table 4*.

**Table 3: Characteristic outputs obtained in the proposed scheme**

Samples	$S$ (nm/RIU)	$Q$	FWHM (nm)	LoD (RI)	FOM (RIU)
DI water	657	2050	10	$1.107 \times 10^{-9}$	65.7
Vibrio Cholera	680	1248	10	$1.784 \times 10^{-9}$	68.0
E Coli	700	919	7	$2.379 \times 10^{-9}$	100
Shigella flexneri	700	739	6	$3.0 \times 10^{-9}$	116.6
Salmonella	700	698	6	$3.19 \times 10^{-9}$	116.6

The results of this proposed work is compared with the previously published reports and shows significant improvements as shown in *table 4*.

**Table 4: Comparison of the proposed work with recent literature**

Ref	Sensor type	Size ( $\mu m^2$ )	$Q$	$S$ (nm/RIU)	Applications
[2]	Biosensor	$19 \times 12$	4856	388	Cancer cells detection
[6]	Biosensor	$R = 200$	---	149	Salmonella detection
[10]	Biosensor	---	416	1.55	E. coli Sensing
[15]	Biochemical Sensor	$6 \times 7$	---	35 and 9.4	Bio-chemical detection
[21]	RI Sensor	$12 \times 12$	4581	1146	Gas sensing
This work	RI Biosensor	55	1130.8	687	Bacterial sample detection. i.e. Vibrio Cholera, E Coli, Shigella flexneri, Salmonella

## 5. CONCLUSION

The biosensor for the detection of bacterial water is proposed. The ultra-small detection volumes are only required for detection and are detected in their natural form. The corresponding change in resonance wavelength is measured,

which is induced by the molecular interactions. The proposed sensor can detect various species of bacteria in water. The sensor offers very high sensitivity with an excellent light confinement. The device is comparatively compact and also has a high  $Q$ -factor. The device provides label-free, real-time detection with low loss. The sensing characteristics are inspected. The proposed sensor is lightweight, and can be fabricated as a lab-on-chip sensor.

## 6. ACKNOWLEDGEMENT

Authors want to thank Prof. Preecha Yupapin, Full Professor, Ton DucThang University (TDTU), Ho Chi Minh City, Vietnam and, Dr. Bhuvneshwer Suthar, Assistant Professor in the Physics department of MLB Government College, Rajasthan, India and for his valuable discussions.

## REFERENCES

- [1] Sulabh, L. Singh, S. Jain, and M. Kumar (2019), "Optical Slot Waveguide with Grating-Loaded Cladding of Silicon and Titanium Dioxide for Label-Free Bio-Sensing," *IEEE Sensors Journal*, vol. 19, no. 15, pp. 6126-6133.
- [2] S. Jindal, S. Sobti, M. Kumar, S. Sharma, and M. Pal (2016), "Nanocavity-Coupled Photonic Crystal Waveguide as Highly Sensitive Platform for Cancer Detection," *IEEE Sensors Journal*, vol. 16, no. 10, pp. 3705-3710.
- [3] P. Sharma, and P. Sharan (2015), "Design of photonic crystal based ring resonator for detection of different blood constituents," *Optics Communications*, vol. 348, pp. 19-23.
- [4] S. Sahu, J. Ali, and G. Singh (2017), "Refractive index biosensor using sidewall gratings in dual-slot waveguide," *Optics Communications*, vol. 402, pp. 408-41.
- [5] S. Kumar et al. (2021), "MoS<sub>2</sub> Functionalized Multicore Fiber Probes for Selective Detection of Shigella Bacteria Based on Localized Plasmon," *Journal of Lightwave Technology*, vol. 39, no. 12, pp. 4069-4081.
- [6] P. Sharma, and P. Sharan (2015), "Design of Photonic Crystal-Based Biosensor for Detection of Glucose Concentration in Urine," *IEEE Sensors Journal*, vol. 15, no. 2, pp. 1035-1042.
- [7] B. Rappazet al. (2005), "Measurement of the integral refractive index and dynamic cell morphometry of living cells with digital holographic microscopy," *Optics Express*, vol. 13, no. 23, pp. 9361.
- [8] R.A. Flynn et al. (2005), "Two-Beam Optical Traps: Refractive Index and Size Measurements of Microscale Objects," *Biomedical Microdevices*, vol. 7, no. 2, pp. 93-97.
- [9] P. Y. Liu et al. (2014), "An optofluidic imaging system to measure the biophysical signature of single waterborne bacteria," *Lab on a Chip*, vol. 14, no. 21, pp. 4237-4243.
- [10] B. Painam, R. Kaler, and M. Kumar (2017), "On-Chip Oval-Shaped Nanocavity Photonic Crystal Waveguide Biosensor for Detection of Foodborne Pathogens," *Plasmonics*, vol. 13, no. 2, pp. 445-449.
- [11] S. Kulkarni, N. Khan, P. Sharan, and B. Ranjith (2020), "Bacterial Analysis of Drinking Water using Photonic Crystal based Optical Sensor," 2020 7th International Conference on Computing for Sustainable Global Development (INDIACom), pp. 186-191, doi: 10.23919/INDIACom49435.2020.9083711.
- [12] P. Sharma, and P. Sharan (2015), "An Analysis and Design of Photonic Crystal-Based Biochip for Detection of Glycosuria," *IEEE Sensors Journal*, vol. 15, no. 10, pp. 5569-5575.
- [13] Z. Zhang, et al. (2018), "Plasmonic Refractive Index Sensor with High Figure of Merit Based on Concentric-Rings Resonator," *Sensors (Basel)*, vol. 18, no. 2 pp. 116.
- [14] Mahesh Shankar Pandey, Dr. Virendra Singh Chaudhary (2021), REULEAUX Triangle Shaped MSPA for 5G and WLAN Applications. *IJEER* 9(4), 107-113. DOI: 10.37391/IJEER.090403.

- [15] B. Painam, R. Kaler, and M. Kumar (2016), "Photonic Crystal Waveguide Biochemical Sensor for the Approximation of Chemical Components Concentrations," *Plasmonics*, vol. 12, no. 3, pp. 899-904.
- [16] R. Jannesari, et al. (2016), "High-Quality-Factor Photonic Crystal Ring Resonator with Applications for Gas Sensing," *Procedia Engineering*, vol. 168, pp. 375-379.
- [17] S. Robinson, and R. Nakkeeran 2013, "Photonic Crystal Ring Resonator Based Optical Filters: Advances in Photonic Crystals, Vittorio M. N. Passaro, IntechOpen, doi: 10.5772/54533.
- [18] M. Bahadoran et al. (2014), "Detection of Salmonella bacterium in drinking water using microring resonator," *Artificial Cells, Nanomedicine, and Biotechnology*, vol. 44, no. 1, pp. 315-321.
- [19] A. M. Upadhyaya, M. C. Srivastava, and P. Sharan (2021), "Integrated MOEMS based cantilever sensor for early detection of cancer," *Optik*, vol. 227, 165321.
- [20] R. Geet et al. (2018), "Refractive index sensor with high sensitivity based on circular photonic crystal," *Journal of the Optical Society of America A*, vol. 35, no. 6, pp. 992-997.
- [21] Y. Chen, W. Wang, and Q. Zhu (2014), "Theoretical study on biosensing characteristics of hetero structure photonic crystal ring resonator," *Optik*, vol. 125, no. 15, pp. 3931-3934.
- [22] E. Luan, et al. (2019), "Enhanced sensitivity of subwavelength multibox wavelength microring resonator label-free biosensors," *IEEE Journal of Selected Topics in Quantum Electronics*, vol. 25, no. 3, pp. 1-11.



© 2022 by Rohit Kumar, Gaurav Kumar Bharti and Ranjit Kumar Bindal. Submitted for possible open access publication under the terms and conditions of the Creative Commons Attribution (CC BY)

license (<http://creativecommons.org/licenses/by/4.0/>).